



Modelling of Modular Multilevel Converter Based Electric Drives

M. Venkatesh¹, T.Sai Tharun², K.L.Raviteja², D.V.Laxman², M.Narayana²

¹Assistant Professor, Dept of EEE, Avanthi Institute of Engineering and Technology, Vizianagaram

²UG Student, Dept of EEE, Avanthi Institute of Engineering and Technology, Vizianagaram

To Cite this Article

M. Venkatesh, T.Sai Tharun, K.L.Raviteja, D.V.Laxman and M.Narayana. Modelling of Modular Multilevel Converter Based Electric Drives. International Journal for Modern Trends in Science and Technology 2023, 9(03), pp. 278-283. <https://doi.org/10.46501/IJMTST0903043>

Article Info

Received: 28 February 2023; Accepted: 23 March 2023; Published: 27 March 2023.

ABSTRACT

This paper presents a control scheme for the modular multilevel converter (MMC) to drive a variable-speed ac machine, especially focusing on improving dynamic performance. MMC topology essentially requires advanced control strategies to balance energy and suppress the voltage pulsation of each cell capacitor. This paper proposes a control strategy for the robust dynamic response of MMC even at zero output frequency employing leg offset voltage injection. The ac machine has been driven from standstill to rated speed without excessive cell capacitor voltage ripples utilizing this proposed strategy.

KEY WORDS: Multi-Level Inverter, Electric Drives, PWM Technique and Harmonics.

1. INTRODUCTION:

A MODULAR multilevel converter (MMC) with focus on high-power medium voltage ac motor drives is presented. The use of an MMC makes it possible to save bulky reactive components in a medium-voltage motor drive application, such as a line-transformer, harmonic filter, and dc-link reactor. Compared with conventional medium voltage source converters, the MMC has a modular structure made up of identical converter cells. Because it can easily provide higher number of voltage level for medium voltage applications, the quality of the output voltage waveform is better. In addition, because of the modular structure it has advantages, such as easy maintenance and assembly. Theoretically, the magnitude of the cell voltage fluctuation is proportional

to magnitude of the output phase current and inversely proportional to operating frequency. For this reason, special effort is demanded to drive the ac machine through MMC, which requires considerable starting torque and low-speed steady state operation. In recent studies of and the principles and algorithms for ac motor drives with the MMC have been introduced. However, they did not address the actual control strategies, such as changing output frequency, including standstill and covering load torque disturbance. The energy balancing control is one of the main issues of an MMC system. In many literatures the energy balancing controls of an MMC that uses circulating current control and modulation scheme have been introduced. The leg offset voltage is used to regulate the circulating current and has little effect on ac

and dc terminal voltages. The conventional balancing controls need the circulating current controller that produces the leg offset voltage reference from the input of circulating current references using the proportional and integral (PI) or the proportional and resonant controller.

The energy balancing control is one of the main issues of an MMC system. In many literatures [6]– [10], the energy balancing controls of an MMC that uses circulating current control and modulation scheme have been introduced. The leg offset voltage is used to regulate the circulating current and has little effect on ac and dc terminal voltages. The conventional balancing controls need the circulating current controller that produces the leg offset voltage reference from the input of circulating current references using the proportional and integral (PI) or the proportional and resonant controller. The performance of the circulating current controller has detrimental effects on the dynamics and complexity of the balancing control. Therefore, to improve the balancing performance by increasing bandwidth of the balancing controller, this paper proposes a balancing control method without the circulating current controller. Therefore, in the view point of capacitor voltage balancing, the leg offset voltage can be directly obtained with no phase delay due to the circulating current controller. Therefore, the bandwidth of balancing controller based on the direct voltage injection method can be extended more than that based on the circulating current controller. In addition, the difference between the cell voltages can be reduced faster. As a result, from the perspective of the control dynamics and control complexity, the proposed leg offset voltage injection method is better and simpler than the conventional circulating current injection method. Furthermore, the injecting frequency of leg offset voltage injection method can be increased more than that of current injection method, because of the extended bandwidth of the proposed method. Therefore, owing to the high-frequency injection with the proposed method, the fluctuation of cell capacitor voltage can be minimized compared with circulating current injection method.

LITERATURE SURVEY

Lesnicar and R. Marquardt the wind turbine, generator and converter are usually in the nacelle on the top of the

tower, but the grid step-up transformer is placed at the bottom and Electric power is transmitted down by the generator through cables of high current rating which are expensive. For the THD reduction of WECS (Wind Energy Conversion System) 17 level MMC (Modular Multi level Converter) technique is used. The MMC is one of the most promising converter topologies for high-voltage applications, especially for high-voltage direct-current (HVDC) transmission systems. This study presents power electronics solution in this MMC based on a PMSG (Permanent Magnet Synchronous Generator) design a MMC voltage source converter is developed to synthesize a high sinusoidal output voltage. In this system a LC Filter is used for the low order harmonic reduction. A set of simulation results conducted in Simulink environment.

M. Hiller discusses a transformer less shunt static compensator (STATCOM) based on a modular multilevel converter (MMC). It introduces a new time-discrete appropriate current control algorithm and a phase-shifted carrier modulation strategy for fast compensation of the reactive power and harmonics, and also for the balancing of the three-phase source side currents. Analytical formulas are derived to demonstrate the accurate mechanism of the stored energy balancing inside the MMC. Various simulated waveforms verify that the MMC based STATCOM is capable of reactive power compensation, harmonic cancellation, and simultaneous load balancing, while controlling and balancing all of the DC mean voltages even during the transient states.

Proposed System Configuration:

Figure 1 shows the circuit configuration of an MMC. This topology needs to be controlled by extra balancing strategies. As shown in Figure 1, since the upper and lower arm currents flow through cells in each arm, the corresponding arm currents cause fundamental periodic pulsations of cell capacitor voltages. The voltage pulsation of each cell's capacitor is mostly affected by the output phase current and output frequency.

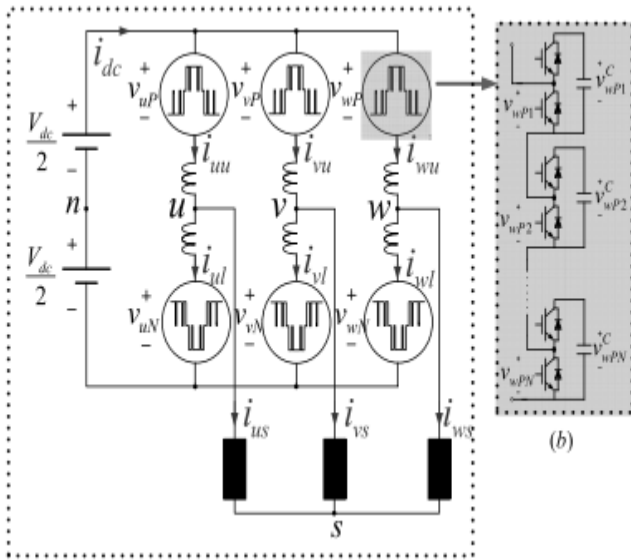


Figure 1: Circuit configuration of the MMC

The cascaded cell modules are shown in Figure 1 in detail. In Figure 1, i_{xu} and i_{xl} are the upper and lower arm currents, respectively, and i_{xs} is the output phase current where x' represents the u -, v -, or w -phase. The output phase current, i_{xs} , and circulating current, i_{x0} , are calculated from the upper and lower arm currents described 1 and 2. Therefore, the arm currents can be deduced as 5.3 ad 5.4, according to the decoupled control scheme in [8] and [11]

$$c = i_{xu} - i_{xl} \quad (1)$$

$$i_{x0} = \frac{i_{xu} + i_{xl}}{2} \quad (2)$$

$$i_{xu} = \frac{1}{2} i_{xs} + i_{x0} \quad (3)$$

$$i_{xl} = -\frac{1}{2} i_{xs} + i_{x0} \quad (4)$$

The leg offset voltage, v_{x0} , produces a circulating current defined as (5), where R and L stand for the resistance and inductance of an arm inductor when all arm inductors in MMC are assumed to be identical. From the voltage relationships along the x -phase loop, the upper, and lower arm voltage references are denoted as 6 and 7, respectively, where V_{dc} is the dc-link voltage, and v_{xP} and v_{xN} are the upper and lower arm voltages, respectively. The common mode voltage, v_{sn} , is the voltage difference between nodes s' and n' , and v_{xs} is the phase voltage, which is $v_{xs} = V_m \cos(\omega st)$. A detailed mathematical description of the relationships in an MMC is given in 10.

$$v_{x0} = (R + L \frac{d}{dt}) i_{x0} \quad (5)$$

$$v_{xN}^* = \frac{V_{dc}}{2} - v_{xs}^* - v_{xn}^* - v_{x0}^* \quad (6)$$

$$v_{xN}^* = \frac{V_{dc}}{2} + v_{xs}^* + v_{xn}^* - v_{x0}^* \quad (7)$$

The instantaneous power of each arm in the x -phase can be deduced as (8) and (9). These two equations must be considered to understand of the proposed balancing control.

$$P_{xp} = v_{xp}^* i_{xu} = \left(\frac{V_{dc}}{2} - v_{xs}^* - v_{xn}^* - v_{x0}^* \right) \left(\frac{1}{2} i_{xs} + i_{x0} \right) \quad (8)$$

$$P_{xN} = v_{xN}^* i_{xl} = \left(\frac{V_{dc}}{2} + v_{xs}^* + v_{xn}^* - v_{x0}^* \right) \left(-\frac{1}{2} i_{xs} + i_{x0} \right) \quad (9)$$

In addition, the upper and lower arm energy can be calculated by 10 and 11 respectively. Each arm energy is the sum of the cell capacitor energies in the corresponding arm at x -phase leg

$$E_{xp} = \frac{1}{2} C_{cell} \sum_{i=1}^N (v_{xP_i}^c)^2 \quad (10)$$

$$E_{xN} = \frac{1}{2} C_{cell} \sum_{i=1}^N (v_{xN_i}^c)^2 \quad (11)$$

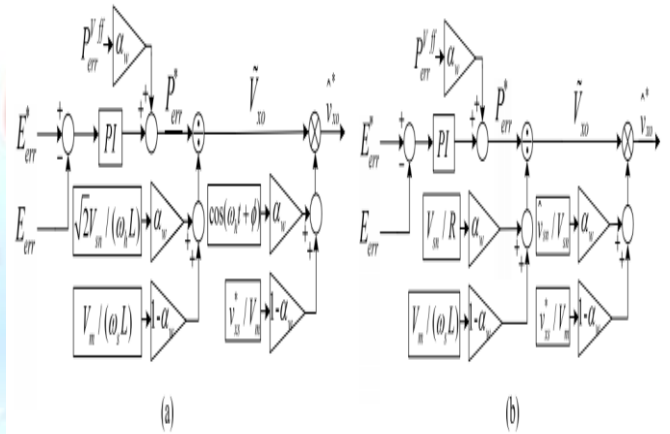


Figure 2: Proposed control scheme for variable-speed drives. (a) Sinusoidal wave voltage injection method. (b) Square wave voltage injection method.

In the case that the sinusoidal wave voltage is injected to both the common mode and the leg offset voltage, the balancing control strategy is shown as a block diagram in Fig. 2(a). E_{err} is the energy difference between the upper and lower arms as in (12). E_{err}^* is the reference of energy difference and should be set as null to keep the balance of the arm energies

$$E_{err} = E_{xp} - E_{xN} = \frac{1}{2} C_{cell} \{ (v_{xP_i}^c)^2 - \sum_{i=1}^N (v_{xN_i}^c)^2 \} \quad (12)$$

PVff err in Fig.2(a) can be derived as (12) by (13)

$$P_{err}^{vff} = \frac{1}{2} V_{dc} i_{xs} - 2v_{dc}^* i_{x0} \quad (13)$$

In the case of the square leg offset voltage injection, on the other hand, the square wave voltage can be injected to both the common mode and the leg offset voltage as

shown in Fig. 2(b). In this case, \hat{v}^{*sn} can be defined by (14) and f_h stands for the frequency of the injected high-frequency voltage

$$\hat{v}_{sn}^* = \begin{cases} -v_{sn} & (0 \leq t < \frac{1}{2f_h}) \\ v_{sn} & (\frac{1}{2f_h} \leq t < \frac{1}{f_h}) \end{cases} \quad (14)$$

Under the assumption that the arm resistance, R , is dominant during each given quasisteady half period, $1/(2f_h)$, \hat{v}^{*xo} can be approximated as (14) from (5), (15), and (14)

$$\hat{v}_{xo}^* \approx \begin{cases} -\frac{R}{2V_{sn}} \left(\frac{1}{2} V_{dc} i_{xs} - 2v_{xs}^* \tilde{i}_{xo} \right) & (0 \leq t < \frac{1}{2f_h}) \\ \frac{R}{2V_{sn}} \left(\frac{1}{2} V_{dc} i_{xs} - 2v_{xs}^* \tilde{i}_{xo} \right) & (\frac{1}{2f_h} \leq t < \frac{1}{f_h}). \end{cases} \quad (15)$$

PVff err in Fig.2(b) can also be derived from (13) using (15) similarly with the case of sinusoidal wave.

Simulink Results:

MMC has been implemented using the time-domain simulation program, PSIM. The number of cells in each arm, N , equals 20. Thus, the system with 120 cells was simulated. Each cell capacitor voltage is controlled as 600 V, and the cell is composed of the half-bridge inverter and the cell capacitance is 6000 μ F. The nearest level modulation is applied to generate the arm voltage references and reduce the switching loss of MMC. From the simulation results the devised method can be applied to high-power medium voltage adjustable drive system based on MMC.

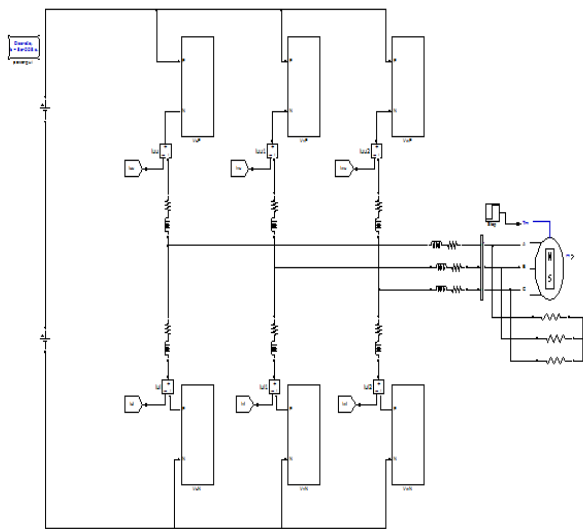
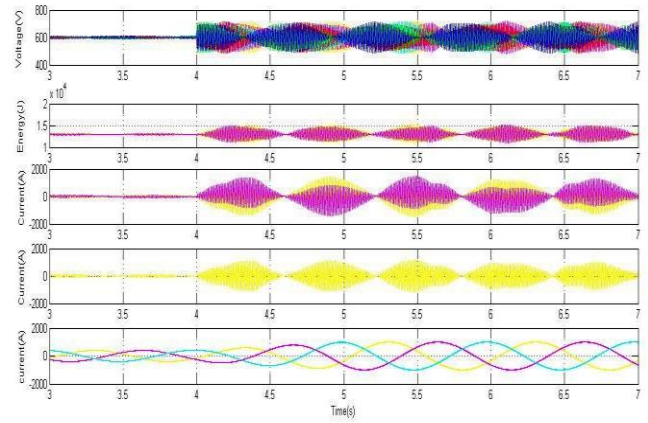
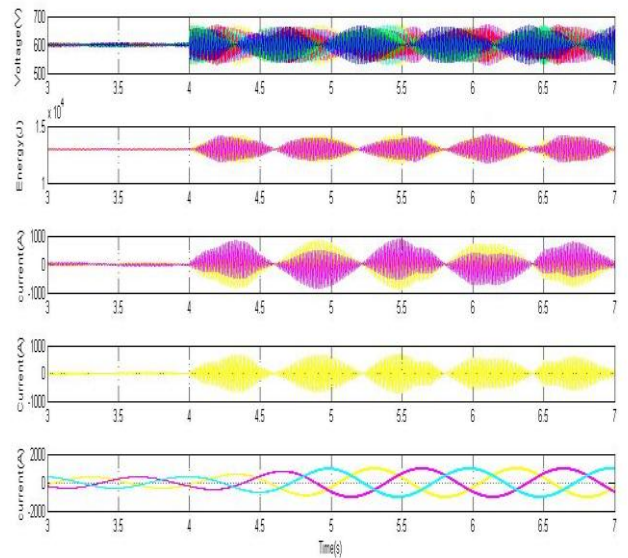


Figure 3: Block diagram of modular multilevel converter



(a)



(b)

Figure 4: Simulation waveform when applying the proposed leg offset voltage injection method with 6r/min speed and step load torque from 10% to 40% of the rated torque. (a) Sinusoidal waveform offset voltage injection. (b) Square waveform offset voltage injection.

The simulation result of the sinusoidal wave leg offset voltage method, and figure 4, shows that of the square wave leg offset voltage method. The high-frequency (100 Hz) voltage is used to balance the arm in low the frequency mode in both sinusoidal and square wave cases. Before 4 s, the PMSM is controlled to be 6 r/min with 10% load torque. At the time point 4 s, the 40% load torque is abruptly applied to the PMSM. Regardless of the impact of step load torque, MMC systems with both sinusoidal and square wave cases have successfully kept the stable operation.

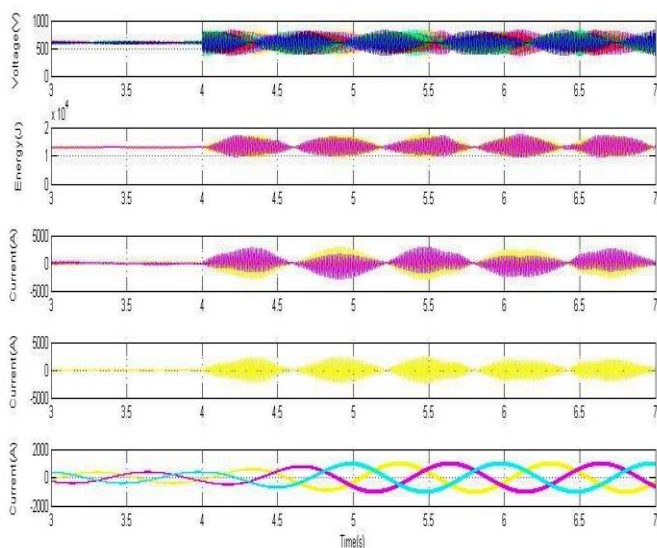


Figure 5: Simulation waveform when applying the conventional circulating current injection method with 6 r/min speed and step load torque from 10% to 36% of the rated torque

Figure 5, the simulation results with the conventional circulating current injection method based on the inner current regulating loop is shown. All operating conditions are identical to those in figure 5 except for the magnitude of the step load torque. For fair comparison between the conventional current injection and proposed leg offset voltage injection methods, the bandwidth for the balancing controller of the two methods is set as the same, and the frequency of the injected component was also set as the same, 100 Hz. The magnitude of the step load torque applied at the conventional current injection method is 36% of the rated torque, which is less than the proposed method test.

CONCLUSION

In this project, a control strategy for variable-speed ac motor drives based on MMC has been presented. To overcome the difficulties of the power balance between cells and arms of MMC over wide operation speed ranges, a direct leg offset voltage injection method has been devised. Utilizing the proposed method, the ripple voltage of each cell of MMC has been kept within allowable bounds under the sudden application of 40% of rated load torque at the extremely low frequency, 1 Hz, which is <2% of rated frequency. Based on the simulation and experimental results, it can be noted that the control performance of the upper and lower arm

energy ripple by the proposed leg offset voltage injection method is better than that by the conventional circulating current injection method with the inner loop. In addition, the variable speed ac motor drive has been proven to work based on the switchover tactic by testing the overall speed including standstill. The analysis and proposed control methods are well agreed by Matlab/Simulink validations.

Conflict of interest statement

Authors declare that they do not have any conflict of interest.

REFERENCES

- [1] Jae-Jung, student Member, IEEE, Hak-Jun Lee, Student Member, IEEE, and Seung-Ki Sul, Fellow, IEEE "Control strategy for improved dynamic performance of variable speed drives with Modular Multilevel Converter"
- [2] A. Lesnicar and R. Marquardt, "An innovative modular multilevel converter topology suitable for a wide power range," in Proc. IEEE Power Tech Conf., Bologna ,Italy ,Jun.2003.
- [3] M. Hiller, D. Krug, R. Sommer, and S. Rohner, "A new highly modular medium voltage converter topology for industrial drive applications," in Proc. 13th Eur. Conf. Power Electron. Appl., Sep. 2009. pp. 1–10.
- [4] G. P. Adam, O. Anaya-Lara, G. M. Burt, D. Telford, B. W. Williams, and J. R. McDonald, "Modular multilevel inverter: Pulse width modulation and capacitor balancing technique," IET Power Electron., vol. 3, no. 5, pp. 702–715, Sep. 2010.
- [5] H. M. Pirouz, M. T. Bina, and K. Kanzi, "A new approach to the modulation and DC-link balancing strategy of modular multilevel AC/AC converters," in Proc. Int. Conf. PEDS, 2005, vol. 2, pp. 1503–1507.
- [6] A. Antonopoulos, K. Ilves, L. Angquist, and H.-P. Nee, "On interaction between internal converter dynamics and current control of high-performance high-power AC motor drives with modular multilevel converters," in Proc. IEEE ECCE, Sep. 2010, pp.4293–4298.
- [7] M. Hagiwara, K. Nishimura, and H. Akagi, "A medium-voltage motor drive with a modular multilevel PWM inverter," IEEE Trans. Power Electron., vol. 25, no. 7, pp. 1786–1799, Jul.2010.
- [8] M.Hagiwara,I.Hasegawa, and H.Akagi,"Start-up and low-speed operation of an electric motor driven by a modular multilevel cascade inverter, "IEEE Trans.Ind. Appl.,vol.49,no.4,pp.1556–1565,Jul./Aug.2013.
- [9] J. Kolb, F. Kammerer, and M. Braun, "Straight forward vector control of the modular multilevel converter for feeding three-phase machines over their complete frequency range," in Proc. 37th Annu. Conf. IEEE Ind. Electron. Soc. IECON, Nov. 2011, pp1596–1601.
- [10] A. Antonopoulos, L. Angquist, S. Norrga, K. Ilves, and H.-P. Nee, "Modular multilevel converter AC motor drives

with constant torque from zero to nominal speed,” in Proc. IEEE ECCE, Sep. 2012, pp. 739–746.

[11] J.-J. Jung, H.-J. Lee, and S.-K. Sul, “Control of the modular multilevel converter for variable-speed drives,” in Proc. IEEE Int. Conf. PEDES, Dec. 2012, pp. 1–6.

[12] L. Angquist, A. Antonopoulos, D. Siemaszko, K. Ilves, M. Vasiladiotis, and H.-. Nee, “Inner control of modular multilevel converters-an approach using open-loop estimation of stored energy,” in Proc. IPEC, Jun. 2010, pp. 1579–1585.

[13] T. Wang and Y. Zhu, “Analysis and comparison of multicarrier PWM schemes applied in H-bridge cascaded multi-level inverters,” in Proc. 5th ICIEA, Jun. 2010, pp. 1379–1383.

[14] S. Rohner, S. Bernet, M. Hiller, and R. Sommer, “Modulation, losses, and semiconductor requirements of modular multilevel converters,” IEEE Trans. Ind. Electron., vol. 57, no. 8, pp. 2633–2642, Aug. 2010.

[15] X. Shi, Z. Wang, L. M. Tolbert, and F. Wang, “A comparison of phase disposition and phase shift PWM strategies for modular multilevel converters,” in Proc. IEEE ECCE, Sep. 2013, pp. 4089–4096.

